Electric Power Systems Research 214 (2023) 108853

Contents lists available at ScienceDirect

Electric Power Systems Research

journal homepage: www.elsevier.com/locate/epsr

A novel line parameter adaptive phasor domain fault location method for double-circuit transmission lines

Yuansheng Liang [a], Zihong Zhang [b], Haifeng Li [a,*], Jiayan Ding [a], Gang Wang [a], Juan Chen [b]

[a] School of Electric Power Engineering, South China University of Technology, Wushan Road No.381, 510640, Tianhe District, Guangzhou, China
[b] Foshan Power Supply Bureau, CSG Guangdong Power Grid Co., Ltd, Fenjiang South Road No.1, 528000, Chancheng District, Foshan, China

ARTICLE INFO

Keywords:
Fault location
Double-circuit transmission lines
Frequency-domain analysis
Line parameter adaptation

ABSTRACT

Phasor domain methods had been commonly used in power transmission line fault location. To improve the accuracy and line parameter adaptive ability of phasor domain fault location, this paper studies a two-terminal phasor domain line parameter adaptive fault location method. First, this paper analyses the convergence issue of original multi-dimensional non-linear fault location equations. Then, by regarding the four complexes consist of fault distance and line parameters as the new unknowns and thereby supplementing a constraint equation about the new unknowns, a quadratic fault location equation set is reconstructed. Furthermore, it is mathematically proven that the four new unknowns are all within the first quadrant. Therefore, the elements in the Jacobian matrix of the reconstructed equation set are all proven to be of symbolic invariance within the solution space. Thus, by using Newton-Raphson method and setting the initial iteration value of the four unknowns to any complexes within the first quadrant, the iteration solution of the reconstructed equation set will converge to the true solution. Finally, electro-magnetic fault simulations are used to evaluate the proposed method. The test results demonstrate that the proposed method is able to guarantee fault location accuracy under different circumstances without knowing line parameters.

1. Introduction

Accurate transmission line fault location is the key to the rapid restoration of faulty lines. The fault location method based on fundamental frequency domain fault analysis has always been one of the main means of AC transmission line fault analysis. Among frequency domain methods, the two-terminal frequency domain method has become a very common fault location method because of its ability to withstand fault resistance [1–6]. Therefore, it has been one of the concerns of fault location researchers to study the two-terminal frequency domain fault location method and strive to improve its accuracy.

There are many factors affecting the fault location of two-terminal frequency domain method. At present, methods are proposed to estimate fundamental phasors for frequency domain method in many researches. Targeting the influence of transient interferences, methods estimate fundamental phasors by utilizing the mathematical relationship between DFT outputs [1,6–9], combining DFT and Prony method [10,11], etc. These methods improve the fundamental phasor estimation accuracy and thereby help to improve the accuracy of phasor domain fault location.

Considering that line parameters may deviate from the given standard parameters due to the influence of climatic and geological conditions of the operation environment, the use of inaccurate line parameters will bring great errors to the fault location results and line parameter estimation for fault location is necessary [12,13]. Methods utilize the voltage and current data before [14–18] or after faults happen [19–22] are proposed. As protective CT has low resolution and measurement accuracy for normal load current, the sampling data of voltage and current before fault in fault transient recording data (FTRD) cannot be directly used to calculate the line parameters. On the other hand, the synchronous measurement data of voltage and current of Phasor Measurement Units (PMUs) during power system normal operation can be used for line parameters estimation. However, it requires smooth information exchange between the Wide Area Measurement System (WAMS) and the Fault Information Analysis System (FIAS), which increases the cost of information system interaction and the difficulty of engineering implementation. In other words, it should be the preferred scheme to use the voltage and current information after fault in the FTRD for line parameter adaptive fault location [19–22]. In these methods, line parameters and fault distance are regarded as unknowns

* Corresponding author.
E-mail address: lihf@scut.edu.cn (H. Li).

https://doi.org/10.1016/j.epsr.2022.108853
Received 25 May 2022; Received in revised form 13 September 2022; Accepted 30 September 2022
Available online 9 October 2022

to construct multi-dimensional nonlinear equations. Meanwhile, various solution schemes are used to solve the equations, such as least squares method (LSM) [19], simulated annealing algorithm [20], Quasi-Newton method [21], particle swarm optimization (PSO) algorithm [22]. These algorithms improved the global optimization performance and efficiency of solving nonlinear equations. However, due to the strong non-linearity of the fault location equations, the solution of the equations is sensitive to the initial iteration value. Therefore, it is easy to converge to a wrong solution or diverge. Most of these methods restrict the range of line parameters, so as to improve the possibility of converging to the correct solution. To do so, the initial iteration value must be close to the true line parameters, which means the line parameters with certain accuracy is needed to be acquired in advance. Consequently, the line parameter adaptive ability of previous fault location methods still needs to be enhanced.

Therefore, this paper aims to study a two-terminal phasor domain fault location method for HVAC transmission lines without acquiring line parameters. Considering that double-circuit line is the main layout of HVAC transmission lines, this paper focuses on the fault location of double-circuit transmission lines. First, the fundamental phasors of positive sequence phase-phase fault currents and voltages at both transmission line ends are estimated. Based on the long line equation, the line parameter adaptive phasor domain fault location equations of fault distance and line parameters are constructed. Considering the strong non-linearity of the equations, to guarantee convergence of the iterative solution process, this paper regards the four complex terms consist of fault location and line parameters as the new complex unknowns of the equation. In this way, a quadratic nonlinear equation set of four complex unknowns is reconstructed. Furthermore, it is proved that the four complex unknowns are all within the first quadrant. Also, in the solution space of the first quadrant, the Jacobian matrix elements of the reconstructed equation set are of symbolic invariance. Consequently, the reconstructed equation set indicates monotonicity in the solution space, which guarantees convergence to the true solution during nonlinear least-square iteration. Finally, electromagnetic simulation cases are utilized to verify the proposed novel line parameter adaptive phasor domain fault location method.

Comparing to the previous phasor domain fault location methods, the main contributions of the proposed method are listed as follow:

1) The proposed method regards four complex terms as the new unknowns and supplements a constraint equation to reconstruct a quadric fault location equation set. The reconstructed equation set is mathematically proven to be of monotonicity. Therefore, convergence to true solution is guaranteed when using Newton-Raphson method to solve the reconstructed equation set.
2) The proposed method is of strong adaptability. It requires no information about line parameters in advance, setting the initial iterative value of four complex unknowns to any complex number within the first quadrant is able to guarantee that the iteration will converge to the true solution.
3) The proposed method improves the iterative calculations by introducing the four new unknowns and reduces the difficulty of selecting initial iterative value, which enhances the adaptive ability of line parameters.

2. Traditional phasor domain fault location method

2.1. Computation of positive sequence fundamental phasors

Fig. 1 shows the 500 kV HVAC transmission system which contains a double circuit transmission line. The design of complete transposition makes the effect of positive and negative sequence coupling inductance ignorable and thereby the positive sequence networks of two circuits are independent. Therefore, this paper analyses the positive sequence network and construct the phasor domain fault analysis model of two

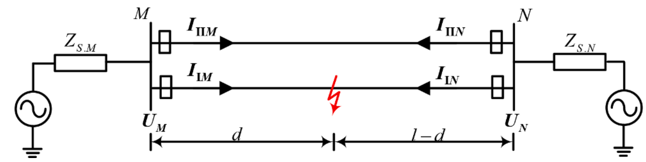

Fig. 1. Schematic diagram of a double-circuit transmission line.

circuits. In order to improve the accuracy of fundamental phasor estimation and thereby guarantee the accuracy of phasor domain fault location, the phasor estimation method proposed in [1] is used to estimate the fundamental phasors of phase voltages and currents at both terminals of both lines. The data time window is from the time fault happened to 1.5 cycles after fault happened and $\boldsymbol{U}_{M\phi}$ (ϕ = A,B,C) is the fundamental phasor of terminal-M phase voltage, $\boldsymbol{U}_{N\phi}$ (ϕ = A,B,C) is the fundamental phasor of terminal-N phase voltage, $\boldsymbol{I}_{IM\phi}$ (ϕ = A,B,C) is the fundamental phasor of terminal-M phase current on line I, $\boldsymbol{I}_{IIM\phi}$ (ϕ = A,B,C) is the fundamental phasor of terminal-M phase current on line II, $\boldsymbol{I}_{IN\phi}$ (ϕ = A,B,C) is the fundamental phasor of terminal-N phase current on line I, $\boldsymbol{I}_{IIN\phi}$ (ϕ = A,B,C) is the fundamental phasor of terminal N phase current on line II.

In order to eliminate mutual inductance coupling effect between phases, the fundamental phasors of phase-to-phase voltages and currents $\boldsymbol{U}_{M\phi\phi}$, $\boldsymbol{U}_{N\phi\phi}$, $\boldsymbol{I}_{IM\phi\phi}$, $\boldsymbol{I}_{IIM\phi\phi}$, $\boldsymbol{I}_{IN\phi\phi}$ and $\boldsymbol{I}_{IIN\phi\phi}$ are calculated by using $\boldsymbol{U}_{M\phi}$, $\boldsymbol{U}_{N\phi}$, $\boldsymbol{I}_{IM\phi}$, $\boldsymbol{I}_{IN\phi}$, $\boldsymbol{I}_{IIM\phi}$ and $\boldsymbol{I}_{IIN\phi}$. Furthermore, the transformation of symmetric component is utilized to calculate the positive sequence phasors $\boldsymbol{U}_M$, $\boldsymbol{U}_N$, $\boldsymbol{I}_{IM}$, $\boldsymbol{I}_{IIM}$, $\boldsymbol{I}_{IN}$ and $\boldsymbol{I}_{IIN}$ for frequency domain fault location.

2.2. The disadvantage of traditional phasor domain fault location method

From Fig. 1, assuming that line I is the faulty line and line II is the healthy line. Utilizing the positive sequence phasors $\boldsymbol{U}_M$, $\boldsymbol{U}_N$, $\boldsymbol{I}_{IM}$, $\boldsymbol{I}_{IIM}$, $\boldsymbol{I}_{IN}$ and $\boldsymbol{I}_{IIN}$ and basing on the long line equation, fault location observation equations of line I and line II can be constructed. In the equations, fault distance d is a real unknown, positive sequence characteristic impedance Z_C and propagation constant γ are complex unknowns.

First, for faulty line I, the voltage along the line is calculated from both terminals and only at the fault point the two calculated voltages are equal:

$$\boldsymbol{U}_M\cosh(\gamma d) - \boldsymbol{I}_{IM}Z_C\sinh(\gamma d) = \boldsymbol{U}_N\cosh[\gamma(l-d)] - \boldsymbol{I}_{IN}Z_C\sinh[\gamma(l-d)] \tag{1}$$

Then, at any point of the healthy line II, the two voltages calculated from both terminals are equal. Taking the points d km and l-d km from terminal-M as the observation point, the following equations can be obtained:

$$\boldsymbol{U}_M\cosh(\gamma d) - \boldsymbol{I}_{IIM}Z_C\sinh(\gamma d) = \boldsymbol{U}_N\cosh[\gamma(l-d)] - \boldsymbol{I}_{IIN}Z_C\sinh[\gamma(l-d)] \tag{2}$$

$$\boldsymbol{U}_M\cosh[\gamma(l-d)] - \boldsymbol{I}_{IIM}Z_C\sinh[\gamma(l-d)] = \boldsymbol{U}_M\cosh(\gamma d) - \boldsymbol{I}_{IIM}Z_C\sinh(\gamma d) \tag{3}$$

Thus, the following multi-dimensional non-linear equation set of d, Z_C and γ can be obtained:

$$\begin{cases} \boldsymbol{f}_1(d,Z_C,\gamma) = \boldsymbol{U}_M\cosh(\gamma d) - \boldsymbol{I}_{IM}Z_c\sinh(\gamma d) \\ \quad - \boldsymbol{U}_N\cosh[\gamma(l-d)] + \boldsymbol{I}_{IN}Z_c\sinh[\gamma(l-d)] = 0 \\ \boldsymbol{f}_2(d,Z_C,\gamma) = \boldsymbol{U}_M\cosh(\gamma d) - \boldsymbol{I}_{IIM}Z_c\sinh(\gamma d) \\ \quad - \boldsymbol{U}_N\cosh[\gamma(l-d)] + \boldsymbol{I}_{IIN}Z_c\sinh[\gamma(l-d)] = 0 \\ \boldsymbol{f}_3(d,Z_C,\gamma) = \boldsymbol{U}_M\cosh[\gamma(l-d)] - \boldsymbol{I}_{IIM}Z_c\sinh[\gamma(l-d)] \\ \quad - \boldsymbol{U}_N\cosh(\gamma d) + \boldsymbol{I}_{IIN}Z_c\sinh(\gamma d) = 0 \end{cases} \tag{4}$$

For the iterative solution of non-linear equation set, comparing to intelligent group optimization algorithms, Newton-Raphson method possesses the advantages of high convergence accuracy and fast solution speed. However, the accuracy of Newton-Raphson method relies heavily on the initial iteration value, especially when solving multi-dimensional equation set with strong non-linearity. Consequently, the situation of convergence to pseudo roots or non-convergence will arise if the line parameters are totally unknown.

3. Line parameter adaptive fault location method based on substituting unknowns

3.1. Fault location equation reconstruction by substituting unknowns and supplementing constraint equations

In the original fault location observation Eqs (1)–(3), the terms related to unknowns d, γ and Z_C are $\cosh(\gamma d)$, $Z_C\sinh(\gamma d)$, $\cosh[\gamma(l-d)]$ and $Z_C\sinh[\gamma(l-d)]$. To avoid the strong non-linearity of the fault location observation equations, assuming that:

$$\boldsymbol{A}=\begin{bmatrix}\boldsymbol{A_1}\\ \boldsymbol{A_2}\\ \boldsymbol{A_3}\\ \boldsymbol{A_4}\end{bmatrix}=\begin{bmatrix}\cosh(\gamma d)\\ Z_c\sinh(\gamma d)\\ \cosh[\gamma(l-d)]\\ Z_c\sinh[\gamma(l-d)]\end{bmatrix} \tag{5}$$

In order to transform the form of unknowns and thereby avoid the strong non-linearity, Eq. (4) is rewritten according to Eq. (5):

$$\begin{cases}\boldsymbol{f_1}(A)=\boldsymbol{U_M A_1}-\boldsymbol{I_{IM}A_2}-\boldsymbol{U_N A_3}+\boldsymbol{I_{IN}A_4}=0\\ \boldsymbol{f_2}(A)=\boldsymbol{U_M A_1}-\boldsymbol{I_{IIM}A_2}-\boldsymbol{U_N A_3}+\boldsymbol{I_{IIN}A_4}=0\\ \boldsymbol{f_3}(A)=-\boldsymbol{U_N A_1}+\boldsymbol{I_{IIN}A_2}+\boldsymbol{U_M A_3}-\boldsymbol{I_{IIM}A_4}=0\end{cases} \tag{6}$$

In Eq. (6), the complex unknowns are $\boldsymbol{A_1}$, $\boldsymbol{A_2}$, $\boldsymbol{A_3}$ and $\boldsymbol{A_4}$ which means the number of equations is less than the number of unknowns. Thus, one more equation should be supplemented. From Eq. (5), the following mathematical relationship of $\boldsymbol{A_1}$, $\boldsymbol{A_2}$, $\boldsymbol{A_3}$ and $\boldsymbol{A_4}$ can be deduced:

$$\begin{aligned}\boldsymbol{A_1A_4}+\boldsymbol{A_2A_3}&=\cosh(\gamma d)\cdot Z_C\sinh[\gamma(l-d)]+Z_C\sinh(\gamma d)\cdot\cosh[\gamma(l-d)]\\ &=Z_C\frac{e^{\gamma d}+e^{-\gamma d}}{2}\,\frac{e^{\gamma(l-d)}-e^{-\gamma(l-d)}}{2}+Z_C\frac{e^{\gamma d}-e^{-\gamma d}}{2}\,\frac{e^{\gamma(l-d)}+e^{-\gamma(l-d)}}{2}\\ &=Z_C\frac{e^{\gamma l}-e^{-\gamma l}}{2}=Z_C\sinh(\gamma l)\end{aligned} \tag{7}$$

Then, using the voltage and current data of the healthy line II, the following equation can be obtained:

$$\begin{cases}\boldsymbol{U_M}\cosh(\gamma l)-\boldsymbol{I_{IIM}}Z_c\sinh(\gamma l)=\boldsymbol{U_N}\\ \boldsymbol{U_N}\cosh(\gamma l)-\boldsymbol{I_{IIN}}Z_c\sinh(\gamma l)=\boldsymbol{U_M}\end{cases} \tag{8}$$

Viewing $\cosh(\gamma l)$ and $Z_C\sinh(\gamma l)$ as unknowns $\boldsymbol{B_1}$ and $\boldsymbol{B_2}$, then Eq. (8) can be rewritten:

$$\begin{cases}\boldsymbol{U_M B_1}-\boldsymbol{I_{IIM}B_2}=\boldsymbol{U_N}\\ \boldsymbol{U_N B_1}-\boldsymbol{I_{IIN}B_2}=\boldsymbol{U_M}\end{cases} \tag{9}$$

According to Eq. (9), B_2 can be calculated and $Z_C\sinh(\gamma l)$ is obtained:

$$Z_C\sinh(\gamma l)=\boldsymbol{B_2}=\frac{(\boldsymbol{U_M^2}-\boldsymbol{U_N^2})}{(\boldsymbol{U_N}\cdot\boldsymbol{I_{IIM}}-\boldsymbol{U_M}\cdot\boldsymbol{I_{IIN}})} \tag{10}$$

Thus, after obtaining $Z_C\sinh(\gamma l)$, Eq. (8) can be rewritten and the supplementary equation is acquired:

$$\boldsymbol{f_4}(A)=\boldsymbol{A_1}\cdot\boldsymbol{A_4}+\boldsymbol{A_2}\cdot\boldsymbol{A_3}-\frac{(\boldsymbol{U_M^2}-\boldsymbol{U_N^2})}{(\boldsymbol{U_N}\cdot\boldsymbol{I_{IIM}}-\boldsymbol{U_M}\cdot\boldsymbol{I_{IIN}})}=0 \tag{11}$$

Thus, the fault location observation equation set can be reconstructed using Eq. (6) and Eq. (11):

$$f(A)=\begin{cases}\boldsymbol{f_1}(A)=\boldsymbol{U_M A_1}-\boldsymbol{I_{IM}A_2}-\boldsymbol{U_N A_3}+\boldsymbol{I_{IN}A_4}=0\\ \boldsymbol{f_2}(A)=\boldsymbol{U_M A_1}-\boldsymbol{I_{IIM}A_2}-\boldsymbol{U_N A_3}+\boldsymbol{I_{IIN}A_4}=0\\ \boldsymbol{f_3}(A)=-\boldsymbol{U_N A_1}+\boldsymbol{I_{IIN}A_2}+\boldsymbol{U_M A_3}-\boldsymbol{I_{IIM}A_4}=0\\ \boldsymbol{f_4}(A)=\boldsymbol{A_1A_4}+\boldsymbol{A_2A_3}-\dfrac{(\boldsymbol{U_M^2}-\boldsymbol{U_N^2})}{(\boldsymbol{U_N}\cdot\boldsymbol{I_{IIM}}-\boldsymbol{U_M}\cdot\boldsymbol{I_{IIN}})}=0\end{cases} \tag{12}$$

Therefore, in Eq. (12), the form of double-circuit transmission line fault location equations are transformed into the form of quadratic non-linear equations.

3.2. Mathematical proof of convergence for the reconstructed fault location equation

The form of quadratic non-linear equation set Eq. (12) is much simpler than that of Eq. (4). Newton-Raphson method is of high convergence accuracy and fast solution speed when solving simple non-linear equations. Therefore, the characteristics of the Jacobian matrix of Eq. (12) should be analyzed. Calculating the partial derivation of $\boldsymbol{A}$, the Jacobian matrix of Eq. (12) is obtained:

$$\boldsymbol{J}(\boldsymbol{A})=\frac{\partial f_i(\boldsymbol{A})}{\partial \boldsymbol{A}}=\begin{bmatrix}\boldsymbol{U_M}&-\boldsymbol{I_{IM}}&-\boldsymbol{U_N}&\boldsymbol{I_{IN}}\\ \boldsymbol{U_M}&-\boldsymbol{I_{IIM}}&-\boldsymbol{U_N}&\boldsymbol{I_{IIN}}\\ -\boldsymbol{U_N}&\boldsymbol{I_{IIN}}&\boldsymbol{U_M}&-\boldsymbol{I_{IIM}}\\ \boldsymbol{A_4}&\boldsymbol{A_3}&\boldsymbol{A_2}&\boldsymbol{A_1}\end{bmatrix} \tag{13}$$

In the Jacobian matrix $\boldsymbol{J}(\boldsymbol{A})$, the elements in the first three rows are fundamental phasors which are constants in the reconstructed equation. The elements in the fourth row are the four complex unknowns of the reconstructed equations. In order to analyse the characteristic of $\boldsymbol{J}(\boldsymbol{A})$, how the four complex knowns change as d, γ and Z_C changes should be analyzed. To do so, the approximate line parameters (γ = 0.0001 + j 0.001 and Z_C = 200 - j10Ω) are selected. By changing the value of d, Z_C and γ separately, the changing rule of the four complexes can be analyzed.

First, the traces of $\boldsymbol{A_1}$ and $\boldsymbol{A_2}$ when d ranges from 0 to 1500 km is are analyzed. As Fig. 2 shows, both traces are always within the first quadrant. As the length of transmission lines is far shorter than 1500 km, the values of $\boldsymbol{A_1}$ and $\boldsymbol{A_2}$ will not exceed the first quadrant.

Then the traces of $\boldsymbol{A_1}$ and $\boldsymbol{A_2}$ when γ changes is are analyzed. Taking d as 0, 100 km, 200 km and 300 km, respectively, when the real part of γ ranges from 0.0001 to 0.01, the traces of $\boldsymbol{A_1}$ and $\boldsymbol{A_2}$ are displayed in Fig. 3. Obviously, $\boldsymbol{A_1}$ and $\boldsymbol{A_2}$ are always within the first quadrant even when the real part of γ deviates from the true value. The traces of $\boldsymbol{A_1}$ and $\boldsymbol{A_2}$ when the imaginary part of γ changes are displayed in Fig. 4. $\boldsymbol{A_1}$ and $\boldsymbol{A_2}$ are always within the first quadrant even when the imaginary part of γ ranges from 0.0001 to 0.005. Thus, it can be concluded that $\boldsymbol{A_1}$ and $\boldsymbol{A_2}$ are always within the first quadrant when γ changes. Similarly, the trace of $\boldsymbol{A_2}$ with Z_C changing is analysed. $\boldsymbol{A_1}$ is not related to Z_C and the traces of $\boldsymbol{A_2}$ when the real and imaginary part of Z_C change are shown in Fig. 5 (a) and (b). As can be seen, the value of $\boldsymbol{A_2}$ is always within the first quadrant.

Generally, the values of $\boldsymbol{A_1}$ and $\boldsymbol{A_2}$ are always within the first quadrant even when the transmission line length and line parameters are far beyond regular values. Also, the possible values of $\boldsymbol{A_3}$ and $\boldsymbol{A_4}$ are the same as those of $\boldsymbol{A_1}$ and $\boldsymbol{A_2}$. Therefore, restricting the range of $\boldsymbol{A_1}$, $\boldsymbol{A_2}$, $\boldsymbol{A_3}$ and $\boldsymbol{A_4}$ to the first quadrant not only caters to the constraint of actual line parameters, but also indicates strong adaptive ability. In the process of iteration, the elements of $\boldsymbol{J}(A)$ are actually the gradient of non-linear curves at iteration value. Thus, the symbolic invariance of these elements indicates that the curves are of monotonicity. In this case, when the zero crossing point of the curve is within solution space, the least square iteration process will certainly converge. If the zero crossing

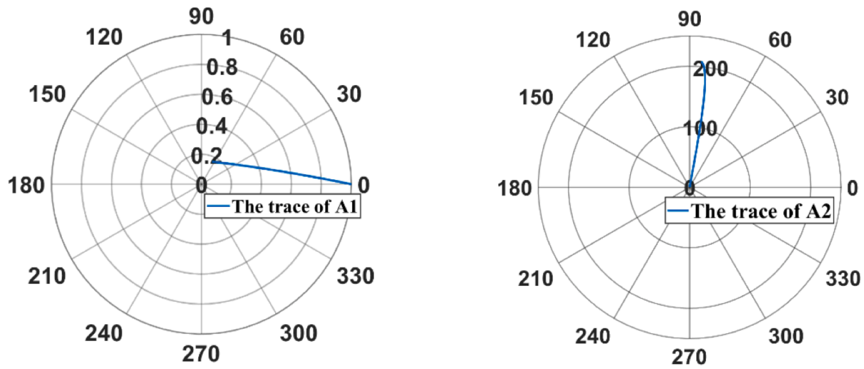

(a) The trace of $\boldsymbol{A_1}$ (b) The trace of $\boldsymbol{A_2}$

Fig. 2. The traces of A_1 and A_2 with d changing.

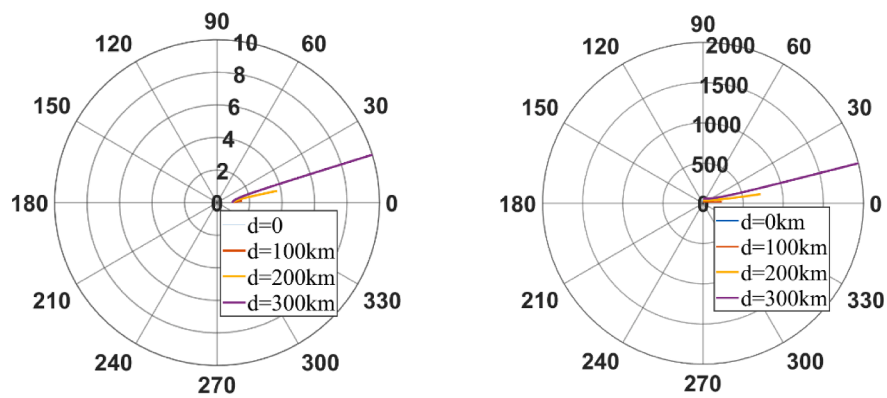

(a) The trace of $\boldsymbol{A_1}$ (b) The trace of $\boldsymbol{A_2}$

Fig. 3. The traces of A_1 and A_2 with the real part of γ changing.

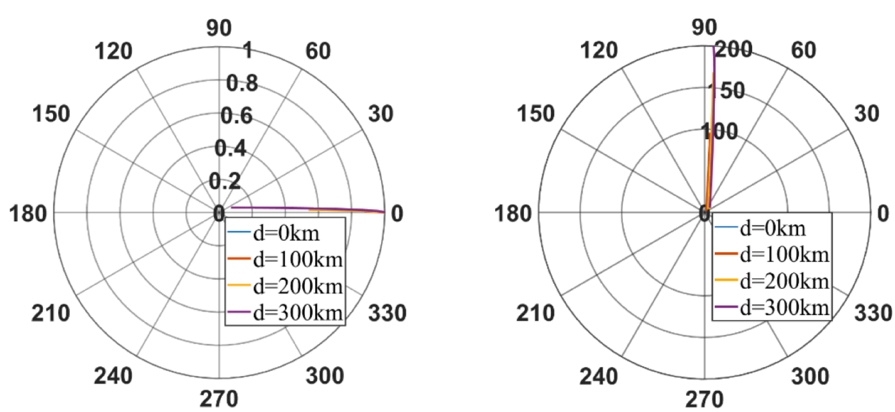

(a) The trace of $\boldsymbol{A_1}$ (b) The trace of $\boldsymbol{A_2}$

Fig. 4. The traces of A_1 and A_2 with the imaginary part of γ changing.

point is where the true solution lies, then convergence to the true solution is guaranteed. In this case, the range of solution space certainly contains the range restricted by regular line parameter values, which means the true solution is within the solution space.

In other words, it can be concluded that:

(1) The solution space of $\boldsymbol{A_1}$, $\boldsymbol{A_2}$, $\boldsymbol{A_3}$ and $\boldsymbol{A_4}$ is within the first quadrant and the elements of $\boldsymbol{J}(\boldsymbol{A})$ are all of symbolic invariance.
(2) Within the first quadrant, the curves of equations in Eq. (12) are of monotonicity. The true solution is unique.

Thus, convergence to true solution is guaranteed when using Newton-Raphson method to solve Eq. (12).

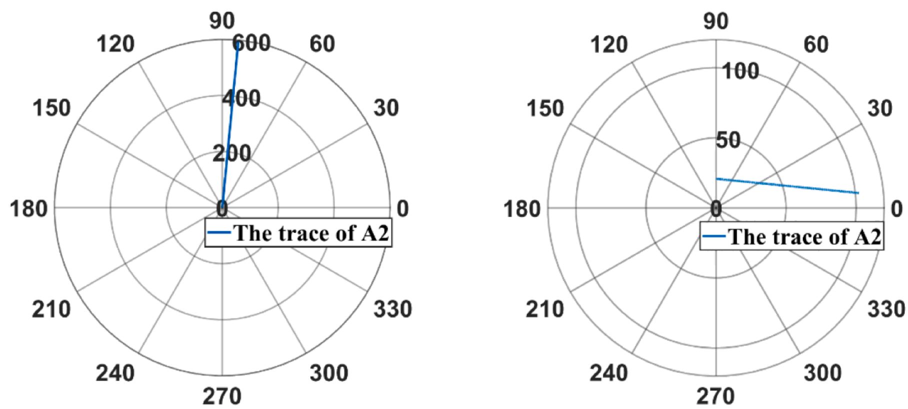

(a) the real part of Z_C changing (b) the imaginary part of Z_C changing

Fig. 5. The trace of A_2 with Z_C changing.

3.3. Solution of the reconstructed fault location equation

Therefore, Newton-Raphson method is used to solve the line parameter adaptive double-circuit transmission line fault location Eq. (12). As the Jacobian matrix of Eq. (12) is already obtained, the Taylor expansion of $f(A)$ at any iteration point $A^{(p)}$ can be calculated and the higher order terms are neglected:

$$f\left(\mathbf{A}^{(\mathbf{p})}\right)+\boldsymbol{J}\left(\mathbf{A}^{(\mathbf{p})}\right)\cdot\Delta\boldsymbol{A}^{(p)}=0 \tag{14}$$

Thus, $\Delta\boldsymbol{A}^{(\mathbf{p})}$ can be calculated using Eq. (14) and the iteration process is continued:

$$\boldsymbol{A}^{(p+1)}=\boldsymbol{A}^{(p)}+\Delta\boldsymbol{A}^{(p)} \tag{15}$$

When $|\Delta\boldsymbol{A}^{(p)}|<\varepsilon$ (ε is an extremely small number), the iteration process is completed and the solution converges at $\boldsymbol{A}^{(p)}$. According to Eq. (5), the fault distance d can be calculated:

$$d=\frac{\operatorname{arcosh}(\boldsymbol{A}_1)/\operatorname{arcosh}(\boldsymbol{A}_3)\cdot l}{\operatorname{arcosh}(\boldsymbol{A}_1)/\operatorname{arcosh}(\boldsymbol{A}_3)+1} \tag{16}$$

In this way, without acquiring line parameters in advance, the fault location observation equation is transformed into the simple quadratic non-linear equations form by substitution of unknowns. Furthermore, in the solution space of the first quadrant, it is mathematically proved that the elements in the Jacobian matrix of the reconstructed equation set indicate symbolic invariance. Consequently, convergence to the true solution is guaranteed when solving the reconstructed equation set by using Newton-Raphson method.

4. Verification of the proposed fault location method by electron-magnetic transient simulation

To verify the proposed double-circuit transmission line fault location method, a 500 kV two-terminal power transmission system model which contains a double-circuit transmission line is constructed using PSCAD/EMTDC. The fault location calculation is programmed in MATLAB. The frequency of the system is 50 Hz. The transmission line model adopts the frequency-dependent J. Marti model, which is more close to the practical transmission lines. The layouts of the transmission system is shown in Fig. 1. The line length l is set to 300 km. Faults are set at 1 km, 5 km, 10 km, 50 km, 100 km, 150 km, 200 km, 250 km, 290 km, 295 km and 299 km away from terminal-M.

Setting the middle of the line as the initial iteration value of fault distance and selecting the iterative initial values of line parameters within the same order of magnitude, the solutions of the original fault location observation equations (i.e., Eq. (4)) acquired by using Newton-Raphson method are listed in Table 1.

It can be seen from Table 1 that three different solution situations arise due to the strong non-linearity of the equation set, which are accurate convergence, convergence to pseudo root and divergence. Therefore, it can be deduced that due to the existence of pseudo root problem in the solution of this kind of multi-dimensional strongly non-linear equations, when the initial value of iteration cannot be close to the true solution, there will be divergences or false convergences, resulting in large deviations of fault location.

In order to verify the effectiveness of the proposed method, utilize the reconstructed observation equation set (i.e., Eq. (12)) to solve the fault distance for the same fault situation. The initial values of real and imaginary parts of $A_1\sim A_4$ are random positive real numbers. The solutions acquired by using Newton-Raphson method and number of iterations (NI) are listed in Table 2.

As can be seen in Table 2, in the same fault situation, the solutions converge to the true fault distance at the NI of 9 or 10 or 11 by using the reconstructed equation set. It shows that the proposed method is insensitive to initial values for unknowns. To further test the accuracy of the proposed method, more fault simulations are carried out and the proposed fault location method is utilized to calculate fault distance under different fault cases. The fault type includes single phase to ground fault, phase to phase fault and three phase fault. For all three types of fault, the fault resistances are set to 0, 50Ω, 100Ω, 200Ω and 300Ω, respectively. The results are listed in Tables 3–5.

It can be derived from Tables 3–5 that the proposed double-circuit transmission line fault location method is able to accurately locate the fault under different circumstance without knowing line parameters. The fault location errors are all less than 0.5 km, thereby the two nearest towers to the fault point can be identified. When the faults occur near line terminals, the fault location errors are still small. On the other hand, fault location results with the existence of fault resistance are an important index for fault location methods. As can be seen from Tables 3–5, with the existence of fault resistance, the proposed method still provides accurate fault location results. When the fault resistance is up to 300Ω under the circumstance of single phase to ground fault, the fault characteristics are obviously weakened and the proposed method is still able to locate the fault accurately. Thus, the proposed fault location method possesses robustness to fault resistance.

Generally, the proposed double-circuit transmission line fault location method possesses strong adaptive ability of line parameters and ample precision in fault location. Moreover, as the accuracy of fault location improves, the proposed method shows robustness to fault resistance which can be up to 300Ω.

Table 1
Solution situation of original non-linear equation set for fault location.

Fault distance(km)	$R_F = 0$		$R_F = 50\Omega$		$R_F = 100\Omega$	
	Result (km)	Error (km)	Result (km)	Error (km)	Result (km)	Error (km)
1	1.27	0.27	0.15	−0.85	0.01	−0.99
5	6.42	0.42	5.33	0.33	1.84	−3.16
10	9.86	−0.14	10.96	0.96	4.18	−5.82
50	150.00	100.00	150.00	100.00	Divergence	/
100	100.10	0.10	99.30	−0.70	150.00	50.00
150	150.00	0	150.00	0	150.00	0
200	Divergence	/	Divergence	/	Divergence	/
250	Divergence	/	150.00	−100.0	Divergence	/
290	0	−290.0	291.26	1.26	293.51	3.51
295	299.99	4.99	Divergence	/	150.00	−145.00
299	933.66	634.66	Divergence	/	150.00	−149.00

Table 2
Solution situation of reconstructed equation set for fault location.

Fault distance(km)	$R_F = 0$			$R_F = 50\Omega$			$R_F = 100\Omega$		
	Result (km)	Error (km)	NI	Result (km)	Error (km)	NI	Result (km)	Error (km)	NI
1	0.96	−0.04	11	1.08	0.08	10	1.10	0.10	10
5	5.07	0.07	9	4.98	−0.02	10	5.26	0.26	9
10	9.88	−0.12	10	9.95	−0.05	10	10.05	0.05	9
50	50.18	0.18	10	49.91	−0.09	9	49.91	−0.09	9
100	99.86	−0.14	9	99.95	−0.05	10	99.93	−0.07	9
150	150.13	0.13	11	150.01	0.01	10	150.00	0.00	10
200	200.07	0.07	10	200.02	0.02	9	199.97	−0.03	11
250	249.84	−0.16	9	250.04	0.04	10	249.96	−0.04	10
290	290.13	0.13	10	290.06	0.06	11	289.93	−0.07	11
295	294.92	−0.08	10	295.01	0.01	10	294.94	−0.06	9
299	299.05	0.05	10	298.99	−0.01	9	298.95	−0.05	10

Table 3
Fault location results of single phase to ground fault cases.

Fault distance(km)	$R_F = 0$		$R_F = 50\Omega$		$R_F = 100\Omega$		$R_F = 200\Omega$		$R_F = 300\Omega$	
	Result (km)	Error (km)	Result (km)	Error (km)	Result (km)	Error (km)	Result (km)	Error (km)	Result (km)	Error (km)
1	0.96	−0.04	1.08	0.08	1.10	0.10	1.11	0.11	1.11	0.11
5	5.07	0.07	4.98	−0.02	5.26	0.26	5.31	0.31	5.37	0.37
10	9.88	−0.12	9.95	−0.05	10.05	0.05	10.11	0.11	10.15	0.15
50	50.18	0.18	49.91	−0.09	49.91	−0.09	49.94	−0.06	49.84	−0.16
100	99.86	−0.14	99.95	−0.05	99.93	−0.07	99.88	−0.12	99.83	−0.17
150	150.13	0.13	150.01	0.01	150.00	0.00	150.01	0.01	150.01	0.01
200	200.07	0.07	200.02	0.02	199.97	−0.03	200.10	0.10	200.18	0.18
250	249.84	−0.16	250.04	0.04	249.96	−0.04	250.04	0.04	250.08	0.08
290	290.13	0.13	290.06	0.06	289.93	−0.07	289.88	−0.12	289.84	−0.16
295	294.92	−0.08	295.01	0.01	294.94	−0.06	294.82	−0.18	294.81	−0.19
299	299.05	0.05	298.99	−0.01	298.95	−0.05	299.08	0.08	299.11	0.11

Table 4
Fault location results of three phase fault cases.

Fault distance(km)	$R_F = 0$		$R_F = 50\Omega$		$R_F = 100\Omega$		$R_F = 200\Omega$		$R_F = 300\Omega$	
	Result (km)	Error (km)	Result (km)	Error (km)	Result (km)	Error (km)	Result (km)	Error (km)	Result (km)	Error (km)
1	0.92	−0.08	0.96	−0.04	0.94	−0.06	0.91	−0.09	0.89	−0.11
5	5.13	0.13	5.03	0.03	4.97	−0.03	4.94	−0.06	5.11	0.11
10	9.64	−0.36	10.03	0.03	10.03	0.03	10.05	0.05	10.07	0.07
50	50.45	0.45	49.90	−0.10	49.88	−0.12	49.87	−0.13	49.88	−0.12
100	99.86	−0.14	99.93	−0.07	99.97	−0.03	99.93	−0.07	99.91	−0.09
150	150.13	0.13	149.99	−0.01	150.00	0.00	149.99	−0.01	150.00	0.00
200	199.92	−0.08	200.06	0.06	200.06	0.06	200.08	0.08	200.06	0.06
250	250.43	0.43	250.09	0.09	250.10	0.10	250.13	0.13	250.12	0.12
290	290.21	0.21	290.03	0.03	289.94	−0.06	289.97	−0.03	289.93	−0.07
295	294.93	−0.07	295.03	0.03	294.93	−0.07	294.93	−0.07	294.86	−0.14
299	299.08	0.08	299.04	0.04	299.06	0.06	299.08	0.08	299.11	0.11

5. Conclusion

This paper presents a two terminal line parameter adaptive frequency domain method for fault location of double-circuit transmission lines. Targeting the issue of divergence or convergence to pseudo roots for strong non-linear equations, the proposed method regards the four complex terms consist of fault location, line parameters as the new complex unknowns of the fault location observation equation. After

Table 5
Fault location results of phase to phase fault cases.

Fault distance(km)	$R_F = 0$ Result (km)	Error (km)	$R_F = 50\Omega$ Result (km)	Error (km)	$R_F = 100\Omega$ Result (km)	Error (km)	$R_F = 200\Omega$ Result (km)	Error (km)	$R_F = 300\Omega$ Result (km)	Error (km)
1	1.28	0.28	1.08	0.08	1.03	0.03	0.95	−0.05	0.92	−0.08
5	4.80	−0.20	5.23	0.23	4.99	−0.01	4.98	−0.02	5.05	0.05
10	10.18	0.18	10.10	0.10	10.03	0.03	10.04	0.04	10.08	0.08
50	50.28	0.28	50.09	0.09	49.94	−0.06	49.90	−0.10	49.94	−0.06
100	99.77	−0.23	99.89	−0.11	99.98	−0.02	100.02	0.02	99.98	−0.02
150	150.12	0.12	149.99	−0.01	149.99	−0.01	150.00	0.00	150.00	0.00
200	199.83	−0.17	200.06	0.06	199.96	−0.04	199.93	−0.07	200.01	0.01
250	249.63	−0.37	249.83	−0.17	249.96	−0.04	249.94	−0.06	249.86	−0.04
290	289.86	−0.14	289.97	−0.03	289.97	−0.03	289.95	−0.05	289.92	−0.08
295	295.12	0.12	295.04	0.04	294.96	−0.04	295.05	0.05	294.92	−0.08
299	298.76	−0.24	298.94	−0.06	298.98	−0.02	299.06	0.06	299.06	0.06

supplementing a constraint equation by utilizing the mathematical relationship between the new complex unknowns, a quadratic non-linear equation set is reconstructed.

It is mathematically proven that the four complex unknowns are always within the first quadrant even if the line parameters and length are far beyond regular value. Thereby, within the solution space of the first quadrant, the elements in the Jacobian matrix of the reconstructed equation set are all of symbolic invariance, which means the reconstructed equation are of monotonicity. Thus, setting the initial iteration value of the four complex unknowns to any complex number in the first quadrant is able to guarantee convergence to true solution. Then, the fault distance can be calculated.

The test of ATP/EMTP-generated signals indicates that the proposed method guarantees accurate convergence and fault location by setting the initial iteration value to any complex in the first quadrant. The adaptive ability to line parameters of the proposed methods is strong. Also, with the improvement of fault location accuracy, the proposed method possesses strong robustness to fault resistance. Even when the fault resistance of single phase to ground fault is up to 300Ω, the fault location accuracy of the proposed fault location method is still high. Therefore, the proposed phasor domain fault location method is of strong robustness, strong adaptive ability of line parameters and high accuracy in fault location of double-circuit transmission lines.

Funding

This work was supported by the Guangdong Basic and Applied Basic Research Foundation under Grant 2021A1515010631.

CRediT authorship contribution statement

Yuansheng Liang: Conceptualization, Data curation, Formal analysis, Funding acquisition, Methodology, Project administration, Resources, Supervision, Writing – review & editing. **Zihong Zhang:** Data curation, Formal analysis, Investigation, Validation, Writing – original draft. **Haifeng Li:** Resources, Supervision, Writing – review & editing. **Jiayan Ding:** Software, Validation. **Gang Wang:** Resources, Supervision. **Juan Chen:** Resources.

Declaration of Competing Interest

The authors declare that they have no known competing financial interests or personal relationships that could have appeared to influence the work reported in this paper.

References

[1] Yuansheng Liang, Zihong Zhang, Haifeng Li, Jiayan Ding, Gang Wang, Lixin Chen, A robust and accurate discrete Fourier transform-based phasor estimation method for frequency domain fault location of power transmission lines, IET Gener. Transm. Distrib. 16 (10) (2022) 1990–2002. May.

[2] C.A. Apostolopoulos, C.G. Arsoniadis, P. Georgilakis, V.C. Nikolaidis, Unsynchronized measurements based fault location algorithm for active distribution systems without requiring source impedances, IEEE Trans. Power Del. 37 (3) (2022) 2071–2082. Jun.

[3] A.G. Augustine, O.D. Naidu, V. Pradhan, R. Sunitha, Improvement in fault location accuracy using Prony based phasor estimation techniques, in: 2019 Fifth International Conference on Electrical Energy Systems (ICEES), 2019, pp. 1–5.

[4] D. Lu, Y. Liu, B. Xie, R. Fan, L. Sun, An improved phasor domain parameter-free fault location algorithm on untransposed lines, in: 2020 IEEE/PES Transmission and Distribution Conference and Exposition (T&D), 2020, pp. 1–5.

[5] Y. Lee, T. Lin, C. Liu, Multi-terminal nonhomogeneous transmission line fault location utilizing synchronized data, IEEE Trans. Power Del. 34 (3) (2019) 1030–1038. Jun.

[6] Yuansheng Liang, Jinmei Guo, Gang Wang, Haifeng Li, A phasor filtering algorithm on eliminating the effect of fault transient components for the frequency domain fault location, in: 2011 International Conference on Advanced Power System Automation and Protection, Beijing, China, 2011, pp. 1507–1512.

[7] K.M. Silva, F.A.O. Nascimento, Modified DFT-based phasor estimation algorithms for numerical relaying applications, IEEE Trans. Power Del. 33 (3) (2018) 1165–1173. Jun.

[8] B. Jafarpisheh, S.M. Madani, S. Jafarpisheh, Improved DFT-based phasor estimation algorithm using down-sampling, IEEE Trans. Power Del. 33 (6) (2018) 3242–3245. Dec.

[9] B. Jafarpisheh, S.M. Madani, S. Mohammad Shahrtash, A new DFT-based phasor estimation algorithm using high-frequency modulation, IEEE Trans. Power Del. 32 (6) (2017) 2416–2423. Dec.

[10] J.K. Hwang, C.K. Song, M.G. Jeong, DFT-based phasor estimation for removal of the effect of multiple DC components, IEEE Trans. Power Del. 33 (6) (2018) 2901–2909. Dec.

[11] M. Tajdinian, M. Allahbakhshi, A.R. Seifi, M.Z. Jahromi, D. Behi, Auxiliary Prony-based algorithm for performance improvement of DFT phasor estimator against transient of CCVT, IET Sci., Meas. Technol. 13 (5) (2019) 708–714. Jul.

[12] C.A. Apostolopoulos, G.N. Korres, A novel algorithm for locating faults on transposed/untransposed transmission lines without utilizing line parameters, IEEE Trans. Power Del. 25 (4) (2010) 2328–2338. Oct.

[13] Mojtaba Nemati, Mehdi Bigdeli, Amir Ghorbani, Hasan Mehrjerdi, Accurate fault location element for series compensated double-circuit transmission lines utilizing negative-sequence phasors, Electr. Power Syst. 194 (2021). May.

[14] J. Fu, G. Song, B. De Schutter, Influence of measurement uncertainty on parameter estimation and fault location for transmission lines, IEEE Trans. Autom. Sci. Eng. 18 (1) (2021) 337–345. Jan.

[15] F.P. Albuquerque, E.C.M Costa, H.B. Liboni Luísa, R.F.R. Pereira, M.C. de Oliveira, Estimation of transmission line parameters by using two least-squares methods, IET Gener. Transm. Distrib 15 (3) (2021) 568–575. Feb.

[16] A. Bendjabeur, A. Kouadri, Mekhilef, Novel technique for transmission line parameters estimation using synchronised sampled data, ET Gener. Transm. Distrib. 14 (3) (2020) 506–515. Feb.

[17] R. Schulze, P. Schegner, R. Živanović, Parameter identification of unsymmetrical transmission lines using fault records obtained from protective relays, IEEE Trans. Power Del 26 (2) (2011) 1265–1272. Apr.

[18] C.S. Indulkar, K. Ramalingam, Estimation of transmission line parameters from measurements, Int. J. Electrical Power Energy Syst. 30 (5) (2008) 337–342. Jun.

[19] Peng Xu, Yuansheng Liang, Gang Wang, A parameter adaptive fault location with two-terminal data for four-parallel transmission lines on the same tower, automation of electric power systems, 34(9) (May 2010) 59–64.

[20] Haifeng Li, Yuansheng Liang, Gang Wang, Songxuan Du, Fault location scheme for transimission line based on simulated annealing and least square algorithm, Proceedings CSU-EPSA 20 (3) (2008) 36–40. Jun.

[21] Zhenya Gao, Research on Transmission Line Fault Location Based on Power Frequency Quality, Guangdong University of Technology, 2011.

[22] Yuansheng Liang, Gang Wang, Haifeng Li, Fault location algorithm based on time-frequency-domain with two terminals asynchronous, Autom. Electric Power Syst. 33 (4) (2010) 62–66. Feb.